Penn Libraries
UNIVERSITY of PENNSYLVANIA

University of Pennsylvania
ScholarlyCommons

Departmental Papers (ESE)

Department of Electrical & Systems Engineering

October 2007

Optical Realization of Bio-inspired Spiking Neurons In Electron Trapping Material Thin

Ramin Pashaie
University of Pennsylvania, raminp@seas.upenn.edu

Nabil H. Farhat
University of Pennsylvania, farhat@seas.upenn.edu

Follow this and additional works at: http://repository.upenn.edu/ese_papers

Recommended Citation

Optical Realization of Bio-inspired Spiking Neurons In Electron Trapping Material Thin

Abstract

A thin film of electron-trapping material (ETM), when combined with suitable optical bistability, is considered as medium for optical implementation of bio-inspired neural nets. The optical mechanism of ETM under blue light and NIR exposure has the inherent ability at the material level to mimic the crucial components of the stylized Hodgkin-Huxley model of biological neuron. Combining this unique property with high resolution capability of ETM, a dense network of bio-inspired neurons can be realized in a thin film of this infrared stimulable storage phosphore. The work presented here, when combined with suitable optical bistability and optical interconnectivity, has the potential of producing an artificial nonlinear excitable medium analogue to cortical tissue.

Keywords

electron trapping materials, neurons

Optical Realization of Bio-inspired Spiking Neurons In Electron Trapping Material Thin Film

Ramin Pashaie, [1,*] and Nabil H. Farhat,[1,2]

[1]*Department of Electrical and System Engineering, University of Pennsylvania, 200 South 33rd Street, Philadelphia, Pennsylvania 19104-6391, USA*

[2]*Mahoney Institute of Neurological Sciences, University of Pennsylvania, 3450 Hamilton Walk, Philadelphia, PA 19104-6074, USA*

*Corresponding author: raminp@seas.upenn.edu

A thin film of electron-trapping material (ETM), when combined with suitable optical bistability, is considered as medium for optical implementation of bio-inspired neural nets. The optical mechanism of ETM under blue light and NIR exposure has the inherent ability at the material level to mimic the crucial components of the stylized Hodgkin-Huxley model of biological neuron. Combining this unique property with high resolution capability of ETM, a dense network of bio-inspired neurons can be realized in a thin film of this infrared stimulable storage phosphore. The work presented here, when combined with suitable optical bistabillty and optical interconnectivity, has the potential of producing an artificial nonlinear excitable medium analogue to cortical tissue.

OCIS codes: 200.4560, 200.4700, 200.3050, 200.4560

1. Introduction

Neurons are the cells responsible for gathering, processing and storing information. Most neurons commonly function by integrating and transferring information via generation and transmission of action potentials, the so-called neuronal spikes [1]. By controlling a nonlinear ion-exchange process, a stimulated neuron can encode the information in the mean firing rate or in the precise timing of action potentials. [1, 2]. As a result, biological neurons are functionally and structurally complex processing elements (CPEs) in contrast to simple models (e.g. sigmoidal neurons) that are employed in the architecture of most artificial neural nets. It is reasonable to expect that the higher-level computational power of the biological neural networks partly stems from the functional complexity of their processing elements. This functional complexity should be preserved in bio-oriented models that emulate neuronal information processing. Beside this complexity, it has been argued that integration of a large number of massively interconnected CPEs in a VLSI chip can be difficult even when the submicron complementary metal-oxide semiconductor technology is utilized [3]. Here in this paper, we show that both problems can be solved by employing the salient features of the optical mechanism of electron-trapping materials (ETMs).

   Dynamics of ETMs under blue light and near infrared (NIR) exposure has been used to produce optoelectronic neurons that imitate the dendritic response [5] and the pulsating behavior [6] of biological neurons. Pursuing the previous research, in this paper, we reveal a certain duality between the optical mechanism of ETM and the dynamics of biological neurons. We show that a thin film of ETM, when combined with suitable optical bistable device, has the essential mechanisms, at the material level, for duplicating the complexity of neural processing. This model would be able to mimic the dynamics of biological neurons during different phases of the generation of the action potentials. Taking this unique property together with the high-resolution capabilities of ETMs, dense arrays of CPEs can be formed in a thin film of this infrared stimulable storage phosphore.

   In section 2 of this paper, the optical mechanism of ETMs under blue light and NIR

illumination is reviewed. Section 3 is dedicated to the discussion of the functional and the structural duality of these two dynamics: neuron and ETM plus optical bistability. The experimental results are presented in Section 4 and the concluding remarks are summarized in Section 5.

2. Dynamics of ETM under Blue Light and Near Infrared Illumination

Electron-trapping materials, which are employed in the structure of optical computational machines [4, 7, 8], associative memories [9, 10], optical data storage [11, 12], and biological models [5,6,13,14] are alkaline-earth sulfides doped with rare-earth luminescence centers [11]. These rare-earth doped elements add trap energy level within the host band-gap. The atomic band structure and the optical mechanism of ETM is displayed in Fig. 1. Illumination of ETM with blue light (wavelength around 450nm) excites some of the electrons of the valance band and sends them to the conduction level. Part of these excited electrons tunnel to the trap energy level and become trapped-electrons. Blue photons also have enough energy to detrap some of the trapped-electrons and produce orange luminescence. Under constant blue light exposure, the generation and recombination processes of electrons balance and the orange luminescence reaches a saturation level. In addition, in a complete dark room without optical excitation, trapped-electrons remain in the trap energy level for a long time.

The charging characteristic curves of ETM are displayed in Fig. 2(a) where a partially erased ETM is exposed to blue light pulses of different intensities [15]. As the curves indicate, before saturation, the ETM responds almost linearly to a constant blue light illumination. Consequently, before saturation, the intensity of orange luminescence is proportional to the temporal integral of the charging intensity. This functionality is reminiscent to the membrane passive response in a biological neuron [16] and can be used in the modeling of neuron's synapto-dendritic responses, which will be discussed further in next section.

Exposing the ETM to near infrared (NIR) laser (wavelength around 1310nm) de-traps some of the trapped-electrons, some of which return to the ground state by releasing their

extra energy as orange light luminescence at a wavelength around 650nm. The discharging characteristic curves of ETM are shown in Fig. 2(b) where a precharged ETM thin film is exposed to NIR pulses of different intensities. The NIR illumination causes an abrupt jump in the level of orange luminescence; however, the process of discharging becomes slower eventually. When the ETM is simultaneously exposed to the blue and NIR light the intensity of orange luminescence converges, after a short transient response, to a constant value known as the equilibrium-state luminescence of ETM [15]. The intensity of orange luminescence in the equilibrium-state is a function of the intensities of the blue and NIR exposures. An equilibrium-state plane of ETM where contours of constant intensities of orange luminescence are plotted as a function of the blue light and NIR intensities is illustrated in Fig. 3 [15]. We will use the equilibrium-state luminescence of ETM to model the resting potential of biological neurons.

Few mathematical models that govern the dynamics of ETM have been described in the literature [17, 18]. Extending these previous works, we have recently proposed an improved mathematical model for describing the dynamics of ETM under simultaneous blue light and NIR illumination [15]. In this model, evolution of the ETM's luminescence is given by the nonlinear differential equation.

$$\frac{dn}{dt} = \frac{4\xi}{\eta} I_B \sinh^2 \left(\frac{n_s - n}{2\xi I_B} \right) - \frac{4\xi'}{\eta'} I_{NIR} \sinh^2 \left(\frac{n}{2\xi' I_{NIR}} \right). \tag{1}$$

and the intensity of orange light luminescence by,

$$I_O = \alpha n(t) I_B + \beta n(t) I_{NIR}. \tag{2}$$

In these equations I_B and I_{NIR} represent the intensities of blue and NIR light respectively. The I_O is the intensity of orange luminescence. The quentities $\xi, \eta, \xi', \eta', \alpha$ and the β are wavelength dependant parameters of the material, $n(t)$ is the instantaneous density of the trapped-electrons, and n_s is the saturation level of $n(t)$ [15]. For any specified values of

4

the blue and NIR exposures, the intensity of the corresponding orange luminescence can be calculated by these two equations. The equilibrium-state occurs when $dn/dt = 0$ that gives:

$$\frac{4\xi}{\eta} I_B sinh^2 \left(\frac{n_s - n^*}{2\xi I_B} \right) = \frac{4\xi'}{\eta'} I_{NIR} \sinh^2 \left(\frac{n^*}{2\xi' I_{NIR}} \right), \tag{3}$$

$$I_O^* = \alpha n^* I_B + \beta n^* I_{NIR}. \tag{4}$$

The n^* and I_O^* are respectively the density of trapped-electrons and the intensity of orange luminescence in the equilibrium-state. This set of equations can be used for the design and simulation of optical arrangements that utilize ETMs including the bio-inspired optical spiking neuron.

3. Bio-Inspired Neuron in a Thin Film of Electron Trapping Material

The dynamics of a biological neuron consist of five discernable phases: Resting state, initial depolarization, depolarization, repolarization, and hyperpolarization [1,2]. These five phases are produced by the functionality of three different ion channels scattered across the cell membrane: leaky ion channels, neurotransmitter gated ion channels (Ligand ion channels), and voltage gated ion channels. These five phases and the states of the gated ion channels in each phase are displayed in Fig. 5. Comparing the ETM's dynamics with the dynamics of a biological neuron reveals a certain structural and functional parallels that can be used to optoelectronically produce several neuron like functions in an ETM thin film. We study these dualities in the current section.

3.A. Structural Dualities

To draw an analogy a small patch of a biological neuron membrane and a simplified model of the ETM's atomic band structure are shown in Fig. 4. Signaling capabilities of a neuron originate from its ability to vary its membrane potential. The membrane potential is the difference between the electric potential within the cell and the surrounding [2]. This potential

difference is a result of the different concentrations of the potassium and sodium cations in the cell's cytoplasm and the surrounding fluid. The neuron's membrane is not permeable to the ions except through some special proteins embedded in the membrane known as ion channels. The ion channels are selective gates that control the concentration of cations within and outside the cell.

A similarity can be drawn to the energy level structure of ETM. The valance band and the trap energy level are isolated from each other by a potential barrier such that no electronic communication can occur in the medium without optical stimulation. The blue and the NIR photons provide a selective mechanism for transporting electrons between two energy levels. Under simultaneous illumination, the intensity of orange luminescence is a function of the density of electrons in two energy levels and can be controlled by the blue light and NIR exposure. Consequently, in our optical model, the trap energy level and the valance band play the role of the cytoplasm and the surrounding fluid, respectively. Instead of the selective ion channels we take advantage of the blue and NIR wavelengths, and the intensity of orange luminescence is the dual of the membrane potential. The concentration of the sodium ions in the surrounding fluid and the concentration of the potassium ions inside the cell's body are replaced by the density of electrons in the valance band and the density of electrons in the trap energy level, respectively.

3.B.   Resting state

Without any external stimulation, the membrane potential of a biological neuron is at the resting potential. The value of the resting potential is determined by the concentration of the potassium and sodium ions inside and outside the cell. The leaky ion channels in the membrane of a neuron are the channels that are permanently open (Fig. 5(a)). The potassium ions that have higher concentration inside the cell diffuse outside through the leaky ion channels. Diffusion of potassium cations changes the membrane potential and produces an electric force against the diffusion force. These two opposing forces move the potassium

ion concentration and the corresponding membrane potential toward the potassium balance value. Sodium ions follow a similar process. Each of these two ions pushes the value of the resting potential toward its own balance value and the neuron resting potential is the equilibrium state of this ionic process that can be theoretically determined by the Nernst equation [1, 2].

In the optical model the role of two types of ionic channels is replaced by the ETM sensitivity to two different wavelengths. Leaky ion channels can be modeled by two constant continuous-wave (CW) blue light and NIR illuminations. Blue wavelength plays the role of the sodium ion channels. Illumination of the ETM with the blue light, stimulates electrons of the valance band and sends them to the trap energy level. At first, the blue light illumination decreases the density of the electrons in the valance band and increases the density of the trapped electrons. However, when the population of the trapped electrons increases, the probability of interaction between the blue photons and the trapped-electrons increases as well. Such interactions can transfer enough energy to the electrons to elevate them out of the trap energy level and produce the orange luminescence. As a result, similar to the diffusion and electric forces in biology, two opposing mechanisms are involved in this process: the interaction of the blue photons with the electrons in the valance band which generates trapped-electrons (generation), and the interaction of the blue photons with the trapped-electrons that returns electrons to the valance band (recombination). A constant blue light illumination pushes the intensity of the orange luminescence toward a balance value, which is a function of the intensity of the blue light (saturation levels of the charging characteristic curves in Fig. 2(a)). Same thing happens during the NIR illumination of ETM. The NIR photons can also interact with the electrons in the valance band and trap energy level. However, the NIR photons do not have enough energy to excite the electrons of the valance band up to the conduction energy level. Consequently, the balance value of the orange luminescence during NIR illumination is zero. When the ETM is under constant simultaneous blue light and NIR illumination, the intensity of the orange luminescence converges to the

equilibrium-state of these two processes. The equilibrium-state luminescence of ETM,which can be theoretically determined by equations (3) and (4), is the dual of the resting potential in a biological neuron.

3.C. *Initial Depolarization*

In contrast to permanently open leaky ion channels, gated ion channels open in response to chemical or electrical stimulations and produce the dendritic response and the neuronal firing. An external stimulation originated from other neurons or sensory system excites the synapse sites that are distributed throughout the dendritic arbor, and depolarizes the neuron by triggering the neurotransmitter gated ion channels. Opening of these ion channels causes influx of positive sodium ions (Fig. 5(b)), and the result is the generation of an excitatory postsynaptic potential (EPSP) that increases the membrane potential. Most neurons produce a significant postsynaptic depolarization by taking the temporal integral of all EPSPs originated from different dendritic synapses; the process known as the spatial-temporal integration.

In the optical model, depolarization is modeled by blue light illumination. The area of ETM under illumination is the place where the optical neuron receives external stimuli in form of blue exposures. Any part of this region can be stimulated to produce the orange luminescence. As a result, the area of ETM under illumination is reminiscent to the spatial distribution of the dendritic tree. When ETM is exposed to a blue light pulse, the density of trapped electrons increases and in a complete dark medium, as mentioned earlier, trapped electrons remain in the trap energy levels. If one exposes the ETM to another blue light pulse, the density of the trapped electrons increases further. Hence, for low blue light exposures the density of trapped electrons and the intensity of orange luminescence of ETM is proportional to the temporal integral of the illumination. This behavior is similar to the temporal integration in biological neurons. Consequently, when the emitted orange light is collected by a single detector, the area of ETM under illumination responds as a spatial-temporal

8

integrator to blue light excitation.

3.D. Depolarization

When a neuron is sufficiently depolarized, its membrane potential passes the threshold voltage which causes opening of sodium voltage-gated ion channels. Opening of sodium voltage-gated ion channels leads to a strong influx of sodium ions (Fig. 5(c)). As a result, the membrane potential of the neuron increases abruptly and the neuron fires. After a limited period of time, in the order of milliseconds, some particular proteins undergoes some conformational change and block the voltage-gated sodium ion channels. The opening and closing of sodium voltage-gated ion channels during depolarization can be modeled by a gaussian shaped pulse.

Similar to the initial depolarization, influx of sodium cations is modeled by blue light photon flux (illumination) which increases the density of trapped-electrons. Higher density of trapped-electrons increases the chance of interaction between trapped-electrons and blue photons which increases the intensity of orange luminescence. Consequently, the depolarization phase can be modeled by exposing ETM to an intense blue light gaussian pulse. In order to compare the level of luminescence with the threshold level, an optical bistable device (such as self-electrooptic effect device (SEED) [19] in an all optical design or a programmable unijunction transistor (PUT) combined with a photodetector in an optoelectronic realization [6]) should be utilized. When the level of the luminescence crosses the threshold level this bistable device produces the required signals to initiate the depolarization and repolarization phases.

3.E. Repolarization and Hyperpolarization

Opening of the sodium voltage gated ion channels follows by opening of the voltage-gated potassium ion channels, leading to an efflux of potassium cations that repolarizes the cell (Fig. 5(d)). Finally hyperpolarization of the neuron relative to the resting potential causes the voltage-dependent potassium channels to close and the voltage-dependent sodium channels

to deactivate so that the normal resting potential of the neuron will eventually be reinstalled (Fig. 5(e)). Opening and closing of the potassium ion channels during the repolarization phase has the form of α-function [24].

In the optical model, repolarization is modeled by NIR pulse that has the form of α-function. This NIR pulse depletes the trap energy level and reduces the probability of interactions with trapped electrons. Consequently, the intensity of the orange luminescence drops to a level that could be even less than the equilibrium emission. When this NIR pulse is damped, the intensity of orange luminescence once again returns to the equilibrium state emission.

Repeated generation of action potentials causes repeated efflux of potassium ions and influx of sodium ions which unbalances the ionic concentration of the cell. However, the membrane of a biological neuron contains special trans-membrane proteins, called ionic pumps that maintain the appropriate ion concentrations across the membrane by transferring specific ions against their concentration level. Unlike biology where two cations are involved in the process, the only mobile particles in the optical model are electrons. Consequently and fortuitously, in the optical model there is no need for a mechanism duplicating the function of ion pumps.

The dualities that are studied in this section are summarized in table 1. The dynamics of ETM under blue light and NIR light illumination combined with suitable optical bistability provide mechanisms for: generating an equilibrium state during resting, computing the spatial-temporal integral of the afferent stimulation, and producing a spike when the level of excitation crosses the threshold level.

4. Experimental Results

In order to verify the above observation, an experiment is carried out. Schematic of the optical arrangement is given in Fig. 6. A thin layer of ETM ($SrS : Eu^{2+}, Sm^{3+}$ in this report [20]) deposited on a $25mm \times 25mm$ substrate of quartz is exposed by five different light sources: RB, R-NIR, DB, H-NIR, and EB. The light sources RB, DB, and EB are

bright blue LEDs, and the R-NIR and H-NIR are 1310nm fiber coupled laser diodes. The light sources RB and R-NIR are driven by DC voltages to provide the constant equilibrium state emission that resembles the resting potential. External excitations are applied by blue illumination using the blue LED EB, and the light sources DB and H-NIR are employed to produce the depolarization and hyperpolarization signals.

A mask with a centered aperture covers the ETM panel to define the exposed area of ETM during this experiment. Blue optical filters are placed in front of the blue LEDs to block any possible infrared radiation. Drivers of all light sources are precisely controlled by a microcontroller board (Cygnal 8051F124). An orange optical filter (Semrock LP01-633Rs-25) is placed in front of a cooled avalanche photodiode (APD) module (Hamamatsu CA4477-01) that measures the intensity of orange luminescence. The output voltage of the APD module is connected to a comparator in the microcontroller board and an oscilloscope for display. This comparator compares the level of the orange luminescence to the threshold voltage that is produced by a signal generator. The threshold voltage could be a DC voltage or an alternating signal with a DC offset. Such a neural model can produce a variety of different firing patterns including periodic and chaotic patterns [21, 22]. The microcontroller controls drivers of all light sources and simulates the functionality of an optical bistable device. A thermo-electric cooler decreases the temperature of ETM in order to increase the luminescence of the phosphore [23].

During experiment, the blue LED RB and the NIR laser diodes R-NIR are biased to provide the simultaneous constant CW illumination of intensities $I_B = 30\mu W/cm^2$ and $I_{NIR} = 5mW/cm^2$ form in a kind of "optical bias". These illuminations, in the equilibrium-state, produce a constant orange luminescence, which is detected by the APD module to generate a constant 1V output. Once in the equilibrium-state, the external excitation is applied by a sequence of narrow gaussian blue pulses with peak intensities and half-amplitude durations of $I_B = 10\mu W/cm^2$ and $5ms$, respectively, which are $30ms$ apart that are generated by the blue LED EB. Each pulse increases the population of the trapped-electrons and the

11

corresponding orange luminescence. As a result, the output voltage of the APD increases and moves toward the threshold level. Fig. 7 illustrates the oscilloscope's screen when ETM is stimulated by a sequence of 3 gaussian blue pulses. As shown in Fig. 7, the excitation level of the 3 gaussian pulses is insufficient for the intensity of orange luminescence to cross the threshold level. Therefore, the intensity of orange luminescence returns to the resting state after the last pulse. On the other hand, exciting the ETM with a sequence of 4 similar gaussian blue pulses produces enough trapped-electrons to enable the intensity of orange luminescence to reach the threshold. When the APD voltage crosses the threshold level the depolarization process begins by exposing ETM to an intense gaussian blue light pulse of peak intensity and half-duration of $I_B = 25\mu W/cm^2$ and $5ms$, respectively, using the blue LED DB. After a small delay of few milliseconds the repolarization process starts by exposing the ETM panel to an α-function shaped NIR pulse of peak intensity $I_{NIR} = 5mW/cm^2$ and time constant $\tau = 20ms$ [24] produced by the NIR laser diode H-NIR (Fig. 8). After firing, the resting state is eventually reinstalled and the intensity of orange luminescence returns to that of the equilibrium state which was set by light sources RB and R-NIR. As the curves in Fig. 8 implicate, if one stimulates the ETM sufficiently, the ETM fires same as a biological neuron.

5. Discussion and conclusion

The science of artificial neural networks was developed over the last few decades with the hope of building brain-like machines that can imitate the intelligence and other higher-level information processing of brain such as perception and cognition. The extensive endeavors to unravel the mysteries of brain have proved that the computational power of brain is the product of the complex dynamics of a large number of its interconnected processing units (neurons). However, implementation of a microscopic model of brain that incorporates small details of neurons, synapses, dendrites, axons, nonlinear dynamics of membrane patches and ionic channels is prohibitively difficult even with the computational resources and the

nanofabrication technologies available today or predicted for near future. The message conveyed in this article is that we could have a better chance to realize a brain-like machine if we seek for a similar dynamics, for example, in the atomic structure of a material. We studied the optical mechanism of ETMs and the dualities between ETM's dynamics and dynamics of neurons. In order to test our hypothesis, we also performed few experiments. Our experimental results convincingly prove the potential advantages of ETM for duplicating the different phases of the neuronal information processing. Large arrays of optical spiking neurons can be integrated in an ETM thin film by exploiting the high resolution capability of ETM (<100 lp/mm for optically clear polycrystalline ETM thin film) combined with the advantages of recently developed state-of-the-art technologies such as high-speed spatial light modulators and optical bistable devices. Such computing machines can be employed for investigation of a variety of neuronal activities including synchronicity, bifurcation and chaos in the high level cortical processes.

6.   Acknowledgments

References

1. M. F. Bear, B. W. Connors, M. A. Paradiso, *Neuroscience exploring the brain*, Lippincott Williams and Wilkins, (2001).

2. T. P. Trappenberg, *Fundamentals of Computational Neuroscience*, Oxford University Press, (2001).

3. S. Prange, and H. Klar, *Neurobionics: An Interdisciplinary Approach to Substitute Impaired Functions of the Human Nervous System*, H. Both, M. Sami, and R. Eckmiller, eds., Elsvier, Amsterdam, p.225, (1993).

4. S. Jutamulia, G. Stori, J. Lindmayer, W. Seiderman, "Use of electron trapping materials in optical signal processing. 1: parallel Boolean logic," Appl. Opt. **29,** 4806-4811 (1990).

5. Z. Wen, N. Farhat, "Optoelectronic neural dendritic tree processing with electron-trapping materials," Opt. letters, **20**, p. 614-616 (1995).

6. Z. Wen, N. Farhat, "Pulsating neuron producted by electron trapping materials," Opt. letters, **19**, p. 1394-1396 (1994).

7. A. D. McAulay, J. Wang, and C. T. Ma,"Optical dynamic matched filtering with electron trapping devices," in Real-Time Signal Processing XI, J. P. Letellier, ed., Proc. Soc. Photo-Opt. Instrum. Eng. **977,** 271-276 (1988).

8. S. Jutamulia, G. Stori, J. Lindmayer, W. Seiderman, "Use of electron trapping materials in optical signal processing. 2: two-dimensional associative memory," Appl. Opt. **30,** 2879-2884 (1991).

9. A. D. McAulay, J. Wang, and C. T. Ma,"Optical orthogonal neural network associative memory with luminescence rebroadcasting devices," in Proceedings of the IEEE International Conference on Neural Networks (Institute of Electrical and Electronics Engineers, New York, 1989), **2,** 483-485.

10. F. Itoh, K. Kitayama, and Y. Tamura,"Optical outer-product learning in a neural network using optically stimulable phosphor," Opt. Lett. **15,** 860-862 (1990).

11. J. Lindmayer, "A new erasable optical memory," Solid State Technol. **31,** 135-138 (1988).

12. J. Lindmayer, P. Goldmith, K. Gross, "Electron-Trapping optical technology- memory's next generation," Comput. Technol. Rev. **10,** 37-42 (1990).

13. R. Pashaie, N. H. Farhat, "Optical Realization of the Retinal Ganglion Receptive Fields on the Electron-Trapping Material Thin Film," 32rd Northeast Bioengineering Conference. Easton, PA, (2006).

14. R. Pashaie, N. H. Farhat, "Realization of Receptive Fields with Excitatory and Inhibitory Responses on the Equilibrium-State Luminescence of Electron Trapping Material Thin Film", Opt. Lett., **32**, p. 1501-1503, (2007).

15. R. Pashaie, N. H. Farhat, "Dynamics of electron-trapping materials under blue light and near-infrared exposure: a new model", to appear in Journal of the Optical Society of America B, **24**, August (2007).

16. J. Huguenard, and D. A. McCormick, *Electrophysiology of the neuron an iteractive tutorial*, Oxford university press, (1994).

17. Z. Wen, N. Farhat, "Dynamics of electron trapping materials for use in optoelectronic neurocomputing," Appl. Opt., **32,** p. 7251-7265 (1993).

18. Z. Wen, N. Farhat, "Electron trapping materials and electron-beam-addressed electron trapping material devices: an improved model," Appl. Opt., **34,** 5188-5198 (1995).

19. A. L. Lentine, D. Miller, "Evolution of the SEED technology: Bistable logic gates to optoelectronic smart pixels," IEEE J. Quantum Electronics, **29**, Feb. (1993).

20. The electron-trapping material used for this investigation was furnished by the former Quantex Corporation, Rockville, Maryland.

21. G. Lee, N. H. Farhat, 'The bifurcating neuron network 1, 'Neural Networks, **14,** p. 115-131, (2001).

22. G. Lee, N. H. Farhat, 'The bifurcating neuron network 2: an analog associative memory,' Neural Networks, **15,** p. 69-84, (2002).

23. Z. Hua, L. Salamanca-Riba, M. Wuttig, and P. K. Soltani, "Temperature dependence of photoluminescence in $SrS : Eu^{2+}, Sm^{3+}$ thin films," J. Opt. Soc. Am. B **10,**, p.

1464-1469, (1993).

24. Opening of potassium ion channels during the repolarization is modeled by α-function: $\alpha(t) = At\,exp(-t/\tau)$ where A is the amplitude factor and τ is the time constant.

Biological Neuron	Optical Neuron in ETM Thin Film
Inside the cell	Trap energy level
Outside the cell	Valance band
Dendrites	Area of ETM under illumination
Sodium and Potassium ions	Electrons
Concentration of Potassium ions inside the cell	Density of Electrons in the trap energy level
Concentration of sodium ions outside the cell	Density of electrons in the valance band
Membrane potential	Intensity of the orange luminescence
Leaky sodium ion channels	CW constant blue light illumination (RB)
Leaky potassium ion channels	CW constant NIR illumination (R-NIR)
Chemically gated sodium ion channels	Blue light illumination (EB)
Voltage gated sodium ion channels	Blue light illumination (DB)
Voltage gated potassium ion channels	NIR light illumination (H-NIR)
Axonal hillock	Bistable optical device (e.g. SEED)
Diffusion and electric force	Generation and recombination

Table 1. Summary of dualities between descriptive entities.
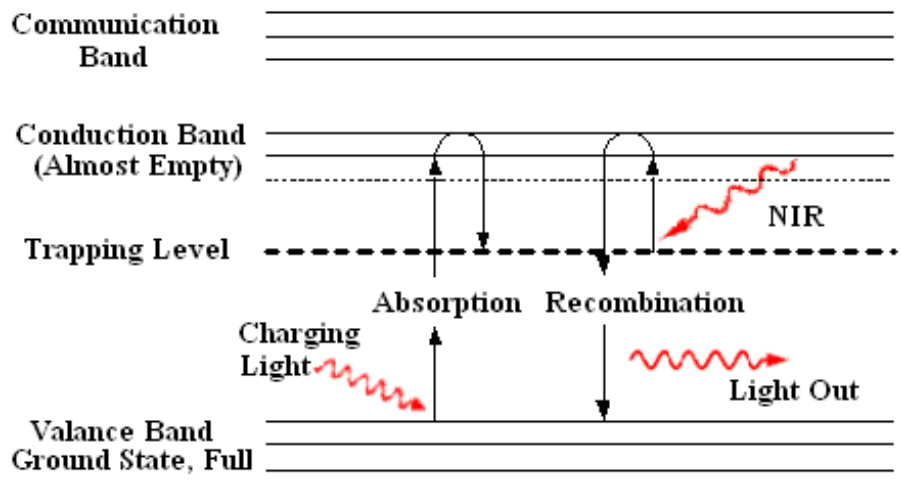
List of Figure Captions

Fig. 1. Optical mechanism of the charging and discharging of ETM. Interaction of blue photons and electrons of valance band excites electrons and sends them to the communication band. Those excited electrons will tunnel to the trap level and become trapped-electrons. NIR photons give sufficient energy to the trapped-electrons to elevate them out of the trapping level, allowing them to return to the valance band and release the stored energy in the form of orange luminescence. [12]

Fig. 2. Experimental and theoretical results of (a) Charging characteristic curves of electron trapping material under different levels of constant blue light illumination. (b) Discharging characteristic curves of electron trapping material under different levels of constant NIR illumination.

Fig. 3. The equilibrium-state plane of a typical ETM sample. Numbers on the contours indicate the intensity of the orange luminescence in nW/cm^2.

Fig. 4. Structural dualities, simplified models of the (a)Neuron membrane, and (b) Energy levels of ETM.

Fig. 5. Status of the ion channels during five different phases of neuron. Leaky ion channels are permanently open. (a) Resting state: All gated ion channels are closed (b) Initial depolarization: neurotransmitter-gated ion channels are open and positive sodium ions penetrate the cell body and increase the membrane potential (c) Depolarization: sodium voltage-gated ion channels are open and sodium ions diffuse to the cell body. (d) Repolarization: sodium voltage gated ion channels get closed eventually when the potassium voltage gated ion channels are open and potassium ions diffuse out of the cell body. (e) Hyperpolarization: The voltage-gated potassium ion channels get closed eventually and the membrane potential returns to the resting potential.

Fig. 6. Schematic of the experimental setup. A thin film of ETM deposited on a thin quartz substrate is exposed by five different light sources: RB, R-NIR, EB, DB, and H-NIR. Among these light sources RB, DB, and EB are blue LEDs and H-NIR and R-NIR are NIR fiber cou-

pled semiconductor lasers. The light sources RB and R-NIR are DC biased to generate the equilibrium state luminescence in the resting state, EB produces signal of the external excitations. Other light sources DB and H-NIR are responsible for producing depolarization and hyperpolarization signals. In the figure acronyms O.F., B.F., and NIR.F stand for Orange, blue and NIR optical filters, respectively.

Fig. 7. Spatio-Temporal integration in ETM. A sequence of 3 gaussian blue light pulses stimulate ETM. Still the level of stimulation is not sufficient to cross the threshold level and the intensity of orange luminescence merges to the resting state after the last blue light pulse.

Fig. 8. Optical spiking neuron. A sequence of 4 gaussian blue light pulses stimulate the ETM. This stimulation is strong enough and the optical neuron fires. After firing, the resting state is reinstated eventually. Two signals on the top are the gaussian shaped blue pulse and the α-function shaped NIR pulse that are dual of opening and closing of sodium voltage gated ion channels during depolarization and opening and closing of the potassium ion channels during repolarization process, respectively.
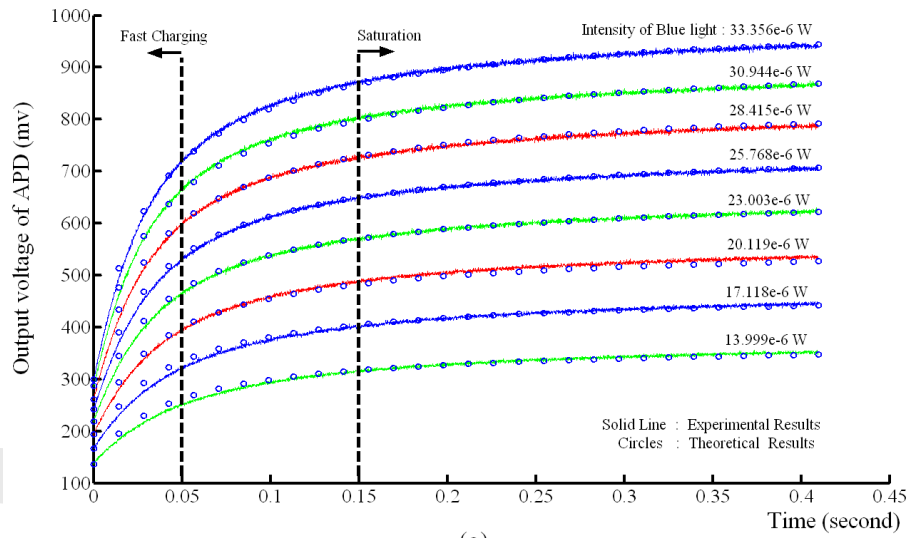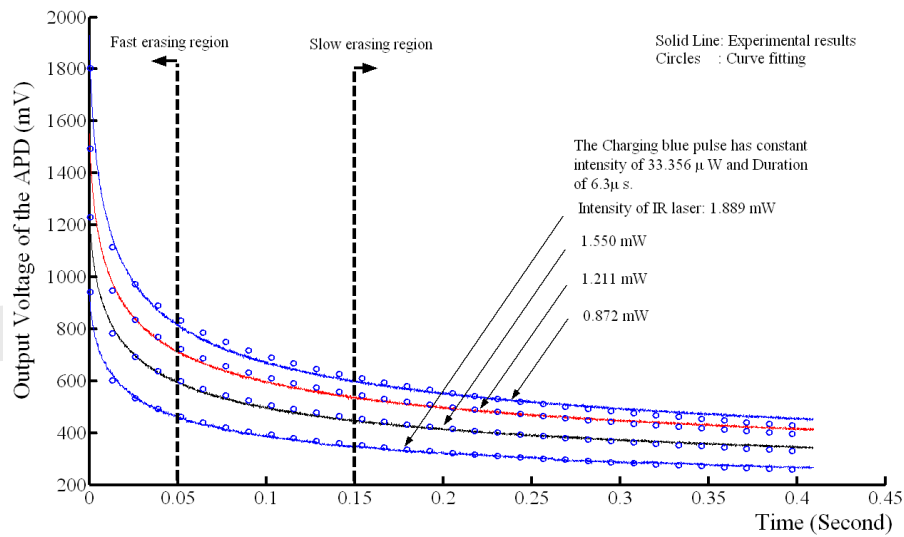
Fig. 1. Optical mechanism of the charging and discharging of ETM. Interaction of blue photons and electrons of valance band excites electrons and sends them to the communication band. Those excited electrons will tunnel to the trap level and become trapped-electrons. NIR photons give sufficient energy to the trapped-electrons to elevate them out of the trapping level, allowing them to return to the valance band and release the stored energy in the form of orange luminescence. [12]

Fig. 2. Experimental and theoretical results of (a) Charging characteristic curves of electron trapping material under different levels of constant blue light illumination. (b) Discharging characteristic curves of electron trapping material under different levels of constant NIR illumination.

21

Fig. 3. The equilibrium-state plane of a typical ETM sample. Numbers on the contours indicate the intensity of the orange luminescence in nW/cm^2.
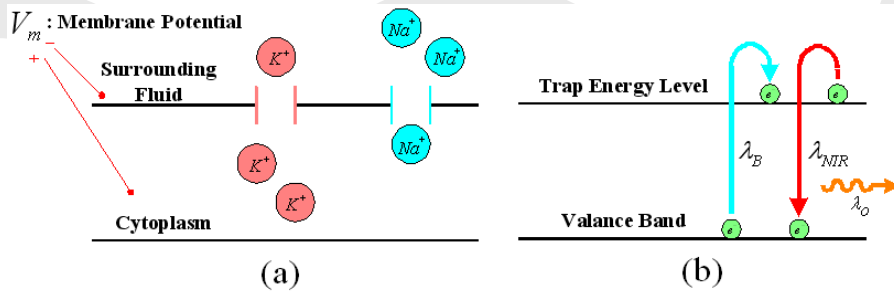
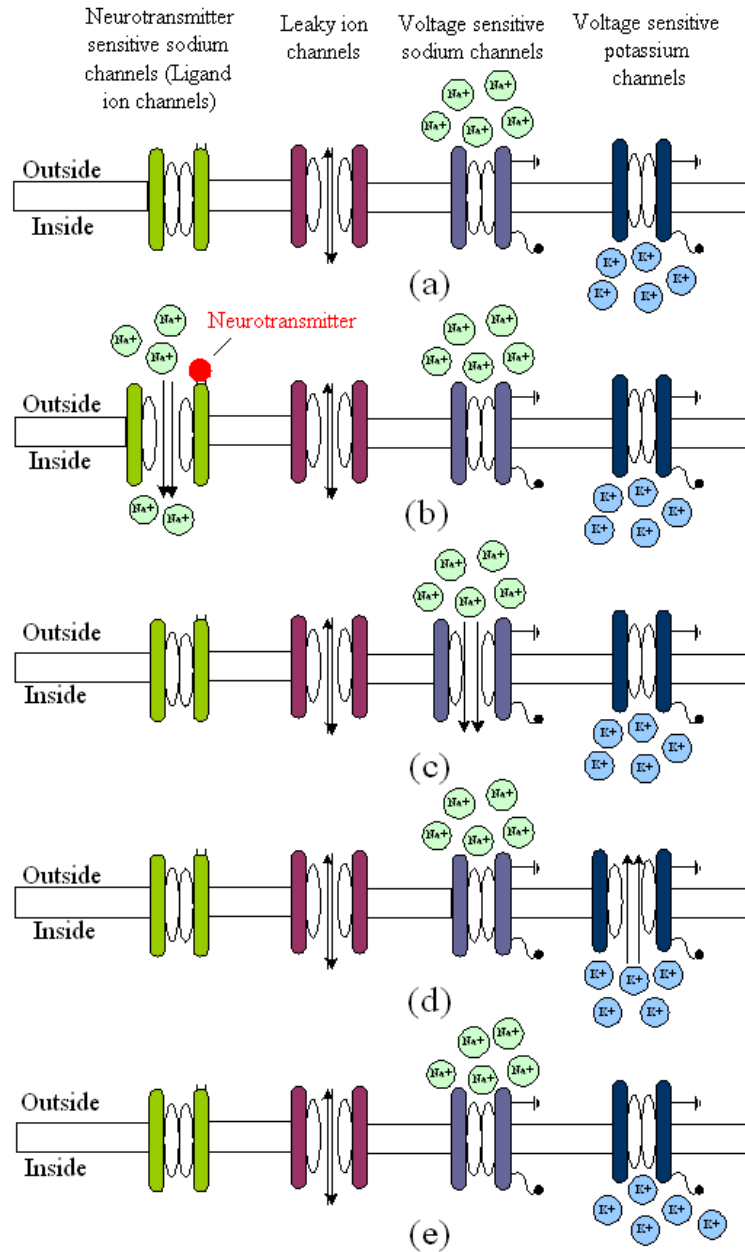Fig. 4. Structural dualities, simplified models of the (a)Neuron membrane, and (b) Energy levels of ETM.

Fig. 5. Status of the ion channels during five different phases of neuron. Leaky ion channels are permanently open. (a) Resting state: All gated ion channels are closed (b) Initial depolarization: neurotransmitter-gated ion channels are open and positive sodium ions penetrate the cell body and increase the membrane potential (c) Depolarization: sodium voltage-gated ion channels are open and sodium ions diffuse to the cell body. (d) Repolarization: sodium voltage gated ion channels get closed eventually when the potassium voltage gated ion channels are open and potassium ions diffuse out of the cell body. (e) Hyperpolarization: The voltage-gated potassium ion channels get closed eventually and the membrane potential returns to the resting potential.
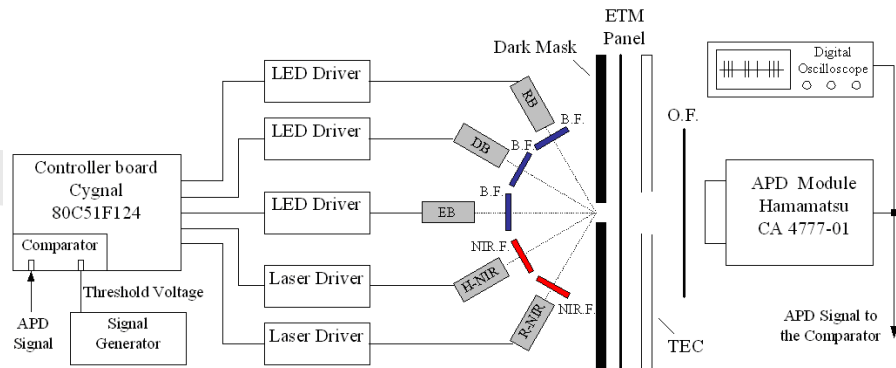
Fig. 6. Schematic of the experimental setup. A thin film of ETM deposited on a thin quartz substrate is exposed by five different light sources: RB, R-NIR, EB, DB, and H-NIR. Among these light sources RB, DB, and EB are blue LEDs and H-NIR and R-NIR are NIR fiber coupled semiconductor lasers. The light sources RB and R-NIR are DC biased to generate the equilibrium state luminescence in the resting state, EB produces signal of the external excitations. Other light sources DB and H-NIR are responsible for producing depolarization and hyperpolarization signals. In the figure acronyms O.F., B.F., and NIR.F stand for Orange, blue and NIR optical filters, respectively.
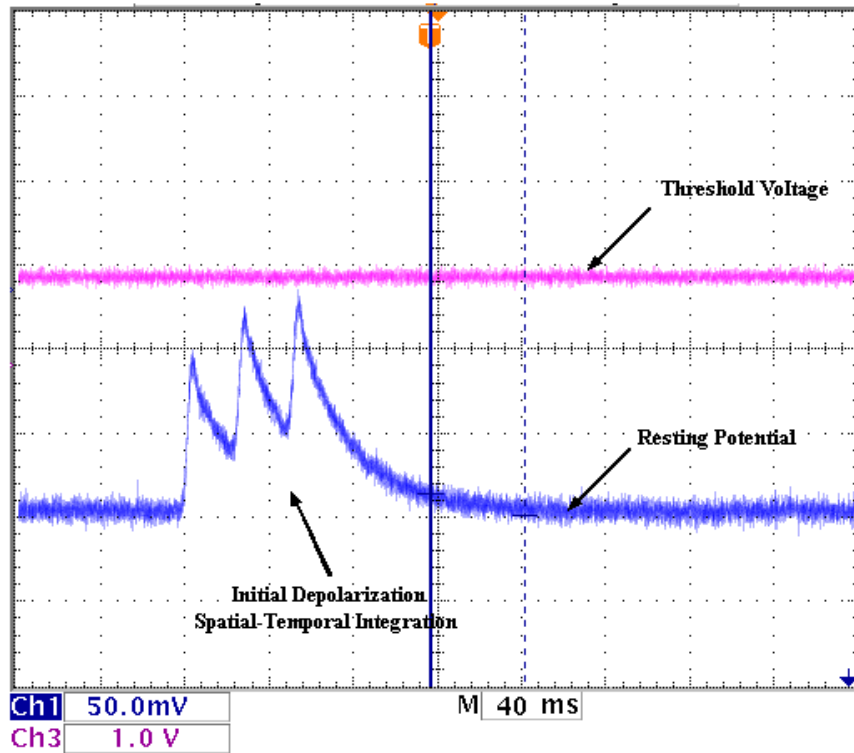
Fig. 7. Spatio-Temporal integration in ETM. A sequence of 3 gaussian blue light pulses stimulate ETM. Still the level of stimulation is not sufficient to cross the threshold level and the intensity of orange luminescence merges to the resting state after the last blue light pulse.
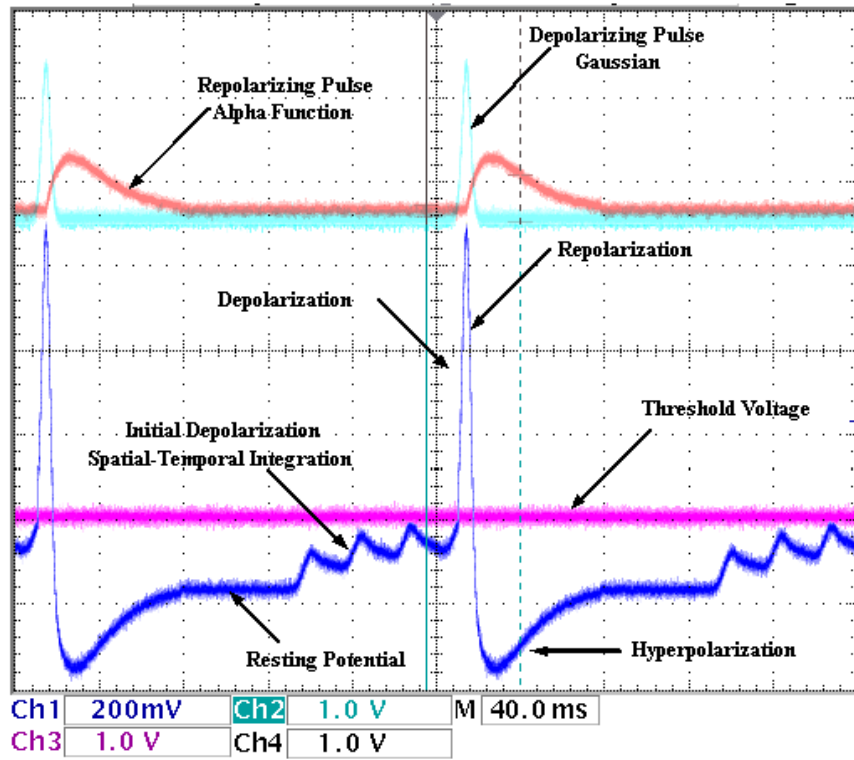
Fig. 8. Optical spiking neuron. A sequence of 4 gaussian blue light pulses stimulate the ETM. This stimulation is strong enough and the optical neuron fires. After firing, the resting state is reinstated eventually. Two signals on the top are the gaussian shaped blue pulse and the α-function shaped NIR pulse that are dual of opening and closing of sodium voltage gated ion channels during depolarization and opening and closing of the potassium ion channels during repolarization process, respectively.